



Available online at www.sciencedirect.com

ScienceDirect

Advances in Space Research 65 (2020) 2052–2061

**ADVANCES IN
SPACE
RESEARCH**
(*a COSPAR publication*)
www.elsevier.com/locate/asr

A comparative study of decision tree, random forest, and convolutional neural network for spread-F identification

Ting Lan, Hui Hu, Chunhua Jiang, Guobin Yang*, Zhengyu Zhao

Department of Space Physics, School of Electronic Information, Wuhan University, Wuhan 430072, China

Received 19 August 2019; received in revised form 19 December 2019; accepted 28 January 2020

Available online 5 February 2020

Abstract

Ionospheric spread-F (SF) is a commonly observed phenomenon of electron density perturbation in the F-layer. The ionospheric irregularities structure has an adverse effect on the propagation of electromagnetic waves in the ionosphere. The automatic identification of ionospheric spread-F and statistical study of the formation of spread-F are of great significance to the study of the physical mechanism of ionospheric inhomogeneity and for prediction of ionospheric irregularities. In this paper, we describe and implement three automatic identification methods of spread-F based on machine learning: decision tree, random forest, and convolutional neural network (CNN). The performance of these automatic identification methods was verified using a large set of test data. Results show that the accuracy of all three methods on identifying ionograms with spread-F exceeded 90%. After comparing the results of the three methods, we found that the decision tree method was the simplest and with the structure easiest to be understood, and it required the shortest interpretation time. In terms of the identification results, the random forest method provided better results than the decision tree method, and the CNN method was the best at accurately identifying ionograms with spread-F.

© 2020 COSPAR. Published by Elsevier Ltd. All rights reserved.

Keywords: Ionograms; Spread-F; Automatic identification; Decision tree; Random forest; Convolutional neural network

1. Introduction

Spread-F (SF), ionospheric irregularity, is a common nighttime phenomenon in the F-layer of the ionosphere in equatorial and low-latitude regions. It causes amplitude and phase fluctuations of electromagnetic waves that pass through the layer, and seriously affects the quality of radio wave communications propagating through the ground-to-space link. For this reason, it is important to study the generation mechanism and predict the occurrence of SF to reduce its influence on shortwave and satellite-to-earth communication. The equatorial ionospheric SF formation mechanism has been studied extensively (Dungey, 1956; Fejer and Kelley, 1980; Sultan,

1996; Fejer et al., 1999), leading to better understanding of the generation and evolution of irregularities in the equatorial ionosphere. The pre-sunset enhancement of the eastward electric field caused an increase in the vertical upward $E \times B$ drift, which promoted the growth of Rayleigh Taylor instability (RTI) (Dungey, 1956; Martyn, 1959; Fejer et al., 1999). SF is also generated in the presence of initial ionospheric perturbations as seeding process, such as gravity waves (GWs), and traveling ionospheric disturbances (TIDs) (Woodman and Hoz, 1976; Tsunoda, 2005, 2006; Abdu et al., 2009; Krall et al., 2011). Some phenomena about SF are not fully understood and require more research, such as the mechanism for generating SF in the post-midnight, the generation and development mechanisms of local generated irregularities in low-latitude regions, and the causes of the generation and development of different types of spread-F, such

* Corresponding author.

E-mail address: gbyang@whu.edu.cn (G. Yang).

as range spread-F, frequency spread-F and mixed spread-F (Piggot and Rawer, 1972).

As ionosondes continue to be deployed and accumulate huge amounts of observational data, to manually identify SF from ionograms is a labor-and material-intensive task. To automatically identify SF would greatly facilitate the statistical analysis of the characteristics and physical mechanism of SF. Recent studies of SF relied mainly on the statistics of its morphological features, and the judgment of whether it had occurred was based on certain empirical thresholds associated with those features (Bhaneja et al., 2009; Pillat et al., 2015; Scotto et al., 2018). The description of morphological changes of SF posed a major hurdle in the discrimination. Lan et al. (2018) proposed a method to identify SF based on decision tree. The method uses machine learning method to automatically obtain the decision threshold (the splits at each tree node) which is based on Gini index (Breiman et al., 1984), with reasonably accurate results. However, the unrestricted growth of the decision tree can easily lead to overfitting and degradation of its generalization capability, and to restrict its growth can jeopardize its fitting ability. The performance depends on its pruning, and to optimize the structure requires extensive cross-validation. Breiman (2001) proposed a random forest approach to improve the decision tree method by randomizing the selection of feature variables and the use of training data. A large number of decision trees are generated by means of unrestricted complete splitting to enhance the model's fitting ability. Due to the two randomness on data and features selection, the random forest is not easy to over-fit in the process of learning, and the classification performance is better than that of decision tree. The advantage of these two methods is that the construction of the model does not require a priori knowledge of the distribution of data categories, and learning and classification are simple and fast. The disadvantage is that some feature parameters, which required the knowledge of SF and experience of the researcher, must be extracted in advance. The success of the random forest method may depend on which features to extract. However, since the distribution features of SF in the ionogram are relatively simple, its identification is also easily accomplished with manual extraction of features. The dependence of the decision tree and random forest on features remains, while deep learning (LeCun et al., 2015) has obvious advantages over conventional machine learning in terms of feature extraction and model construction. Deep learning is good at extracting abstract features from input data, and those features have good generalization capabilities. Deep learning does not require manual determination of features, and the process of building a classification model is automatic, which reduces human errors and the dependence on professional knowledge and judgment. Since the features used in deep learning are obtained directly from the ionograms, some a priori features of SF cannot be utilized, so the learning process is more difficult than that of conventional machine learning, and the training time is longer. Besides, a priori knowl-

edge of the distribution of data categories is required for deep learning to obtain a more accurate classification. The convolutional neural network (CNN) is a typical structure of deep learning.

In this paper, we compare the efficiency of the decision tree, random forest, and CNN for SF identification in the ionograms.

2. Dataset

The Wuhan Ionospheric Sounding System (WISS) (Shi et al., 2009) is a portable, low-power, high-performance ionospheric sounding system developed by the Ionospheric Laboratory of Wuhan University. WISS has three detection modes: vertical incidence, oblique incidence, and oblique backscatter detection. In 2013, a WISS station was installed at Pu'er, Yunnan Province, where the ionosonde is carrying the daily sounding. The detection frequency range is 2–20 MHz, and ionogram data are acquired at a five-minute interval. A software tool ionoScaler (Jiang et al., 2017) was used to explore and manually identify ionograms in this study. We used the 95,550 ionogram recorded from January to December 2015 and July 2016 to train and test the three methods. The data recorded in July 2016 data were also used because a large amount of SF occurred in that month. Ionograms were divided into two parts in order to use mutually independent data to train and test the methods used in this paper. The ionograms recorded in the first half of each month in 2015 (47,711 ionograms) were used as the training data. The ionograms in the second half of each month in 2015 and July 2016 (48,839 ionograms) were used as test data. We divided the ionograms into two categories, depending on whether they contained SF. Fig. 1 shows typical ionograms with and without SF.

3. Automatic identification methods for SF

3.1. Introduction of methods

We used three methods to identify SF; these are the decision tree, random forest, and CNN. Decision tree and random forest are conventional machine learning methods in which the feature parameters are extracted first and then used to train the classifier. CNN is a classic method of deep learning. Feature extraction is automatically completed, hence it is not necessary to extract feature parameters first. The three methods and their input parameters are briefly introduced below.

3.1.1. Decision tree

A decision tree is a basic classifier whose two steps are learning and classification. In the learning phase, the decision tree learns to generate a decision tree from a set of training samples that have been classified. In the classification phase, the decision tree obtained from the learning phase is used to classify unclassified data. A decision tree

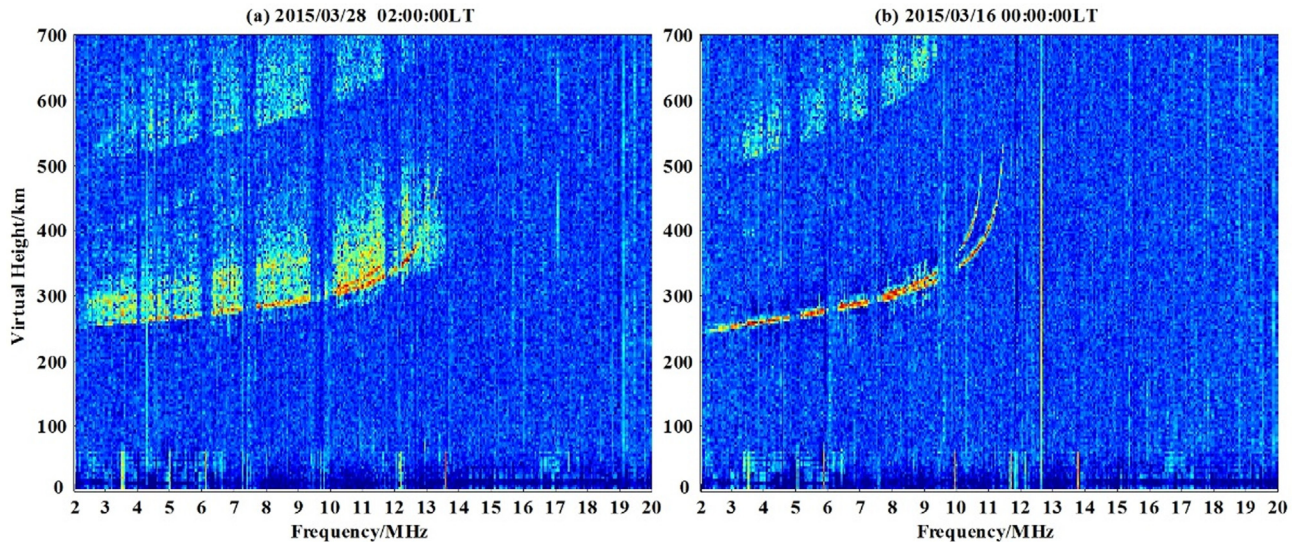


Fig. 1. Typical ionograms with and without SF (a) Ionogram with SF; (b) Ionogram without SF.

has a flowchart-like structure with three parts: internal node, branch, and leaf node. Fig. 2 presented a simple example of decision tree which has four dimensional feature space and two classes. Each internal node represents a test on a feature, each branch is an output of a feature test, and each leaf is the final node that stores the classification classes. A decision tree is intuitive and easy to understand, and its learning and classification steps are simple and quickly implemented. A decision tree must be pruned to avoid overfitting and simplify the tree structure. Based on the feature-selection metric (split criterion), the three main types of decision trees are ID3, C4.5, and CART. We used the CART decision tree (Breiman et al., 1984) to identify SF.

3.1.2. Random forest

Random forest is a classification algorithm proposed by Breiman (2001) based on the bagging idea (Breiman, 1996). It combines multiple weak classifiers (decision trees) to form a stronger classifier. It grows an ensemble of trees

and the final classification is obtained by letting these trees vote for the most popular class. The features of each generated tree are randomly selected at each node, whereas a common CART decision tree uses all the features. So, random forest guarantees the randomness of features. While randomly selecting features, the input training data used to generate each tree consist of a fixed number of training samples extracted from a complete training set by a random sampling with replacement. This ensures the randomness of training samples. Then, a tree is grown on the new training set using random feature selection. Each tree grows to the maximum extent without pruning. Dual randomness enables random forests to resist overfitting, and it enhances the accuracy and generalization capability. Finally, random forest uses multiple trees to make a decision by letting these trees vote for the most popular class. A random forest provides more accurate classifications than a decision tree, but the interpretability is less clear because the features playing an important role are unknown.

3.1.3. Convolutional neural networks

CNN is a classic, widely-used structure in deep learning. First proposed by LeCun et al. (1998), CNN have gained maturity in applications and are now capable of text recognition, facial recognition, image classification, and medical image classification (Lawrence et al., 1997; Ciresan et al., 2011; Li et al., 2014; Kang et al., 2017). The local connection, weight sharing, and pooling operation of CNN can effectively decrease the number of neural network parameters, reduce the network's complexity, bestow a certain degree of invariance to translation distortion and scaling, and enable easy training and optimization. Training and classification is automatic, and does not require the artificial determination of which parameters to extract, or the extraction of image feature values before training step.

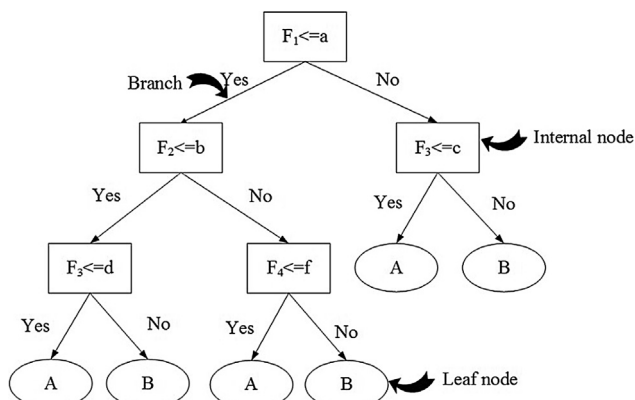


Fig. 2. A simple example of decision tree. The F_i are feature values; a, b, c, d , and e are the thresholds and A and B are class labels.

CNN can automatically and efficiently extract sophisticated abstract features to simplify image classification and enhance classification accuracy.

CNN generally consists of three parts: an input layer; a hidden layer comprising one or more convolutional layers, pooling layers, and fully connected layers; and an output layer. Through forward propagation, CNN can obtain the output value of the network. Through backpropagation, it can adjust the weight of each network layer according to error to realize the adaptive learning and training process of the network.

3.2. Implementation of methods

To facilitate comparison of results, all training data used in the three methods, as well as the test data, came from the same set of ionograms. Both training data and test data are manually classified into two types, ionograms with SF and ionograms without SF.

3.2.1. SF identification based on decision tree

The schematic diagram of the decision tree method is shown in Fig. 3.

To identify SF, one must first extract the model input feature parameters from the ionogram. Pre-processing of the ionogram includes de-noising, F-layer trace extraction, and feature parameter extraction. Feature parameter extraction is implemented automatically based on image-projection methods. After studying the literature on the characteristics of ionospheric SF and the spatial distribution characteristics of SF in ionograms, we extracted 10 features from each ionogram (Lan et al., 2018). The feature parameters are shown in Table 1. We constructed the decision tree according to the CART model and pruned using cross-validation. The decision tree is shown in Fig. 4.

3.2.2. SF identification based on random forest

Like the decision tree, the random forest cannot directly use the original ionograms data as input parameters. The required feature parameters must be extracted from each ionogram in advance. The random forest and decision tree used the same set of feature parameters, which are shown

Table 1

Input parameters for random forest and decision tree (Lan et al., 2018).

Parameter	Description
Season	spring, summer, autumn, or winter
h'F2	minimum virtual height of F2 layer
fxI	maximum frequency of F2 layer
DON	day or night?
PVF	peak value of frequency projection curve
PVH	peak value of height projection curve
SWF	spread width of frequency
SWH	spread width of virtual height
TAF	total amount of candidate SF points on frequency projection curve
TAH	total amount of candidate SF points on height projection curve

in Table 1. The flowchart for random forest identification is similar to that in Fig. 3, just replacing the decision tree by random forest.

After adjusting the random forest parameters and comparing the output results, the random forest chosen for this study contained 500 decision trees. The maximum allowable number of features for a single decision tree at each split in a random forest is the square root of the total number of features (if the maximum allowable number of features is not an integer, the number is rounded up to the next integer), and the minimum number of leaves is one. After setting the parameters, the training data are used to train the random forest and to obtain the required classification model for testing the test data.

3.2.3. SF interpretation based on CNN

3.2.3.1. Setting input parameters. CNNs use the ionograms data directly as input. The ionogram is represented by a matrix S (M, N). M and N are defined by the following formulas:

$$M = \text{int}[(h'_{\max} - h'_{\min})/\Delta h] + 1$$

$$N = \text{int}[(f'_{\max} - f'_{\min})/\Delta f] + 1$$

where h'_{\max} and h'_{\min} are the highest and lowest virtual height recorded on the ionogram, f'_{\max} and f'_{\min} are the maximum and the minimum of the scanning frequency, respectively;

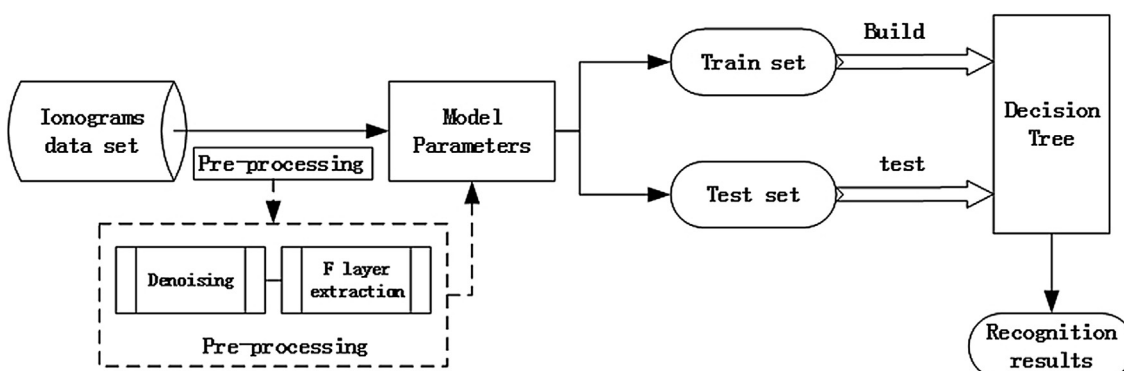


Fig. 3. Overall schematic diagram of SF identification using decision tree.

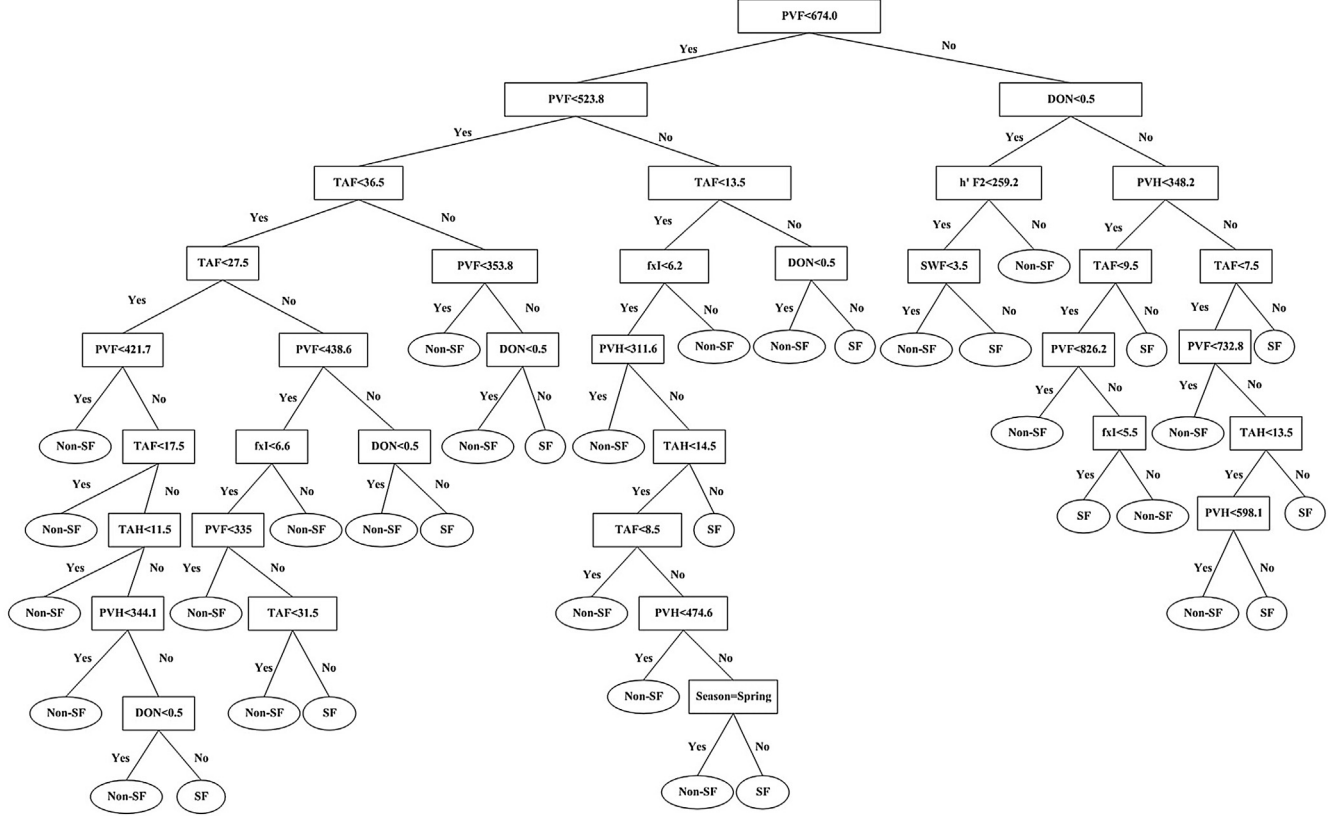


Fig. 4. Decision tree constructed to identify SF using training dataset (Lan et al., 2018).

Δh is the height resolution which has a value of 3.8 km; Δf is the frequency resolution which is 0.05 MHz. Since the trace of the F-layer in the ionogram generally appears in the height range from 180 km to 1,000 km, and the nighttime critical frequency in the Pu'er region is generally less than 15 MHz, so the portion of ionogram which is represented by S (40:260, 1:260) was taken as the useful F layer signal of ionogram and as the input data of the neural network, as shown in Fig. 5, where the area shaded with slanted lines represents the truncated input data.

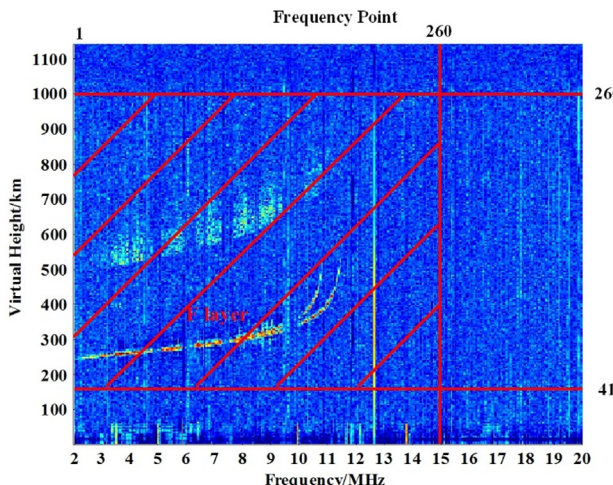


Fig. 5. Extraction diagram for effective data.

Since the number of ionograms with SF is relatively small compared to normal ionograms, a network model trained by unbalanced training samples tends to generalize poorly and to suffer from overfitting when there is great disparity between the distribution probabilities of the two sample groups. It is therefore necessary to expand the ionograms with SF to reduce the imbalance of the sample distribution. Because of the number of ionograms with SF is 3703 in the training set, and the number of ionograms without SF is about 12 times of that with SF in training set, each ionogram with SF is expanded to 12 by parallel displacement in the up, down, left, and right directions. Specifically, the original ionogram is sequentially shifted to the right by 3, 6, 9, 12, 15, and 18 columns, and upward by 2, 4, 6, 8, 10, and 12 rows to generate 12 new ionograms with SF. The expanded and original ionograms are used together as inputs to CNN to train the networks.

3.2.3.2. Network structure. To obtain better interpretation results, we compared the actual interpretation results of various network structures, and chose a CNN structure with four convolutional layers and two pooling layers for this study. The network structure is shown in Fig. 6. As the figure shows, the first few layers of the neural network structure (except the input layer) consist of two convolutional layers (C) and one pooling layer (Max-pooling) alternately connected twice, and then connected to a fully connected layer. The last layer acts as the output layer of

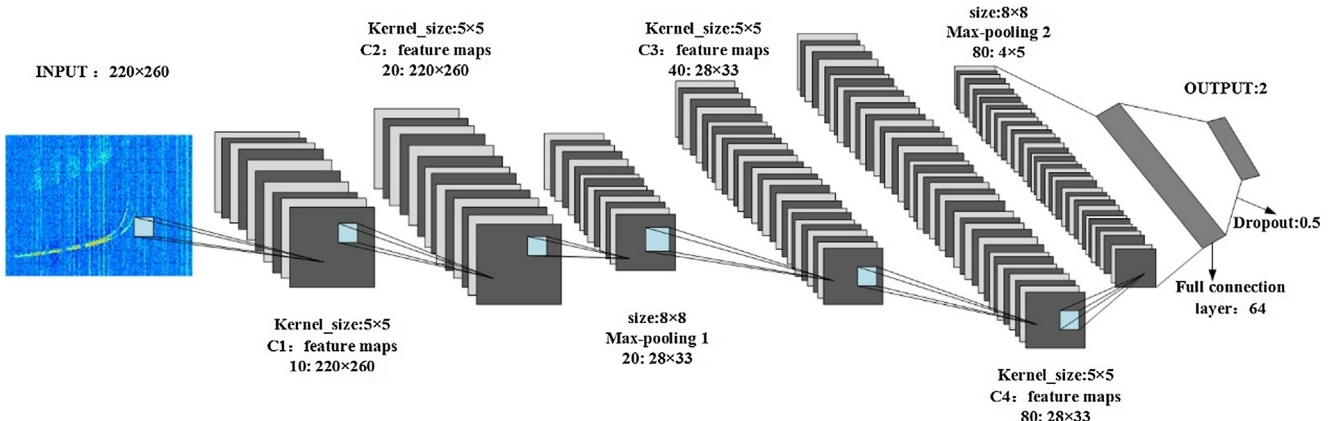


Fig. 6. Structural diagram of neural network.

CNN. In this paper, the size of convolution kernels in all the convolutional layers are 5×5 , and the pooling windows of all the pooling layers are 8×8 .

3.2.3.3. Network training. The neural network training process is the process of minimizing the loss function, which is the objective function of neural network optimization. The loss function used in this paper is defined by the following formulas:

$$\text{loss} = \text{Cross_Entropy_loss} + \lambda \|W\|_2$$

where

$$\text{Cross_Entropy_loss} = - \frac{\sum_{i=1}^n (y_{\text{true_}i} \times \log(y_{\text{cnn_}i}))}{n}$$

$$\|W\|_2 = \|w_1, w_2, \dots, w_{n-1}, w_n\|_2 = \sum_{i=1}^n w_i^2$$

where $y_{\text{cnn_}i}$ represents the predicted value after the i -th training sample enters the CNN, and $y_{\text{true_}i}$ represents the label corresponding to the i -th training sample, n is the total number of training sample. The value of λ is taken to be 0.01. W represents the weight of the CNN to be trained, and $w_i (i = 1, 2, \dots, n)$ represents the i -th value of W .

We used the Adam algorithm (Kingma and Ba, 2015) to optimize the loss function and the identification performance of the network. Adam is a first-order optimization algorithm that can replace the traditional stochastic gradient descent process. It can iteratively update the neural network weights based on the training data.

4. Analysis of SF identification results

We used a set of ionograms independent of the training data to test the accuracy of the three methods. This set of ionograms includes the second half of each month in 2015 and the whole month of July 2016, for a total of 48,839 ionograms, of which 4,476 had SF and 44,363 did not. All the ionograms were classified manually and separated into two categories: with SF and without SF. Feature parameters which were extracted from the ionograms were used as input for the decision tree and random forest. The two methods used the same feature parameters. The iono-

grams for CNN were first cropped into images of size 220×260 according to the method in Section 3.2.3, and these were used as input parameters of the network. The automatic identification results of the three methods were compared with the results of manual interpretation.

In order to compare the performances of the three methods, an index named d was defined on the basis of the criterion used to determine the optimal threshold of a classifier in the ROC curve method (Fawcett, 2006). According to the ROC curve method, the best classifier is the one that has the least value of $d = ((1-TPR)^2 + FPR^2)^{1/2}$, where TPR is the fraction of ionograms with SF that were classified as SF, FPR is the fraction of ionograms without SF that were classified as SF in this study. As a neutral parameter of error cost valuation, index d is useful for unequal classification error costs and is suitable to compare the performances of difference classification methods in this study. Tables 2–4 show the statistical results of SF automatically identified by the decision tree, random forest, and CNN, respectively. The TPR is the percentage value in the first row first column cell of Tables 2–4, and the FPR is the percentage value in the second row second column cell of Tables 2–4. So, the values of the index d for the three methods are calculated, respectively, and the values of d are presented in Table 5. A comparison of Tables 2 and 3 shows that the random forest is slightly more accurate than the decision tree. A comparison of Tables 3 and 4 shows that, in terms of correctly identifying SF in an ionogram with SF, the correct rate of the neural network is 99%. This implies that the neural network is highly accurate in identifying ionograms with SF; however, compared to the decision tree, the neural network has a greater probability for misidentifying ionograms without SF as ones with SF. We can therefore conclude that the neural network sacrifices some of the correct rate for identifying ionograms without SF to maximize the accuracy at identifying ionograms with SF. Table 5 shows that CNN method has the minimum value of d , which demonstrates the CNN is the best method to identify the ionograms with SF. Figs. 7, 8, and 9 show ionograms misidentified by the decision tree, random forest, and CNN methods, respectively.

Table 2

Accuracy rate of decision tree.

	Correct (Correct rate %)	Incorrect (Error rate %)	Total number
With SF	4,039 (TPR = 90.2%)	437 (9.8%)	4,476
Without SF	43,747 (98.6%)	616 (FPR = 1.4%)	44,363
Total number	47,788 (97.8%)	1,051 (2.2%)	48,839

Table 3

Accuracy rate of random forest.

	Correct (Correct rate %)	Incorrect (Error rate %)	Total number
With SF	4,118 (TPR = 92%)	358 (8%)	4,476
Without SF	43,792 (98.7%)	571 (FPR = 1.3%)	44,363
Total number	47,912 (98.1%)	929 (1.9%)	48,839

Table 4

Accuracy rate of convolutional neural network.

	Correct (Correct rate %)	Incorrect (Error rate %)	Total number
With SF	4,436 (TPR = 99.1%)	40 (0.9%)	4,476
Without SF	42,376 (95.5%)	1,987 (FPR = 4.5%)	44,363
Total number	46,812 (95.8%)	2,027 (4.2%)	48,839

Table 5

d values for the three methods.

Method	Decision Tree	Random Forest	CNN
<i>d</i>	0.099	0.081	0.046

After comparing and analyzing the three tables, we conclude the following:

- (1) The random forest method has a higher accuracy rate than the decision tree method. For identifying ionograms with SF, the correct rate of neural network interpretation is much higher than those of the other two methods, but for identifying ionograms without

SF, the neural network performs slightly worse than the other methods.

- (2) In the feature-parameter extraction process, the decision tree and random forest methods require some understanding of the characteristics of SF. The characteristics of spread F are automatically extracted during training step in the neural network, which reduces the requirements of user experience and knowledge. It would be useful for neural network to know the distribution probability of the categories in advance to prevent preferred weighing of categories with higher probability distributions, but an approximate probability can be obtained in the manual interpretation of the training data. Therefore, oversampling or undersampling can compensate for

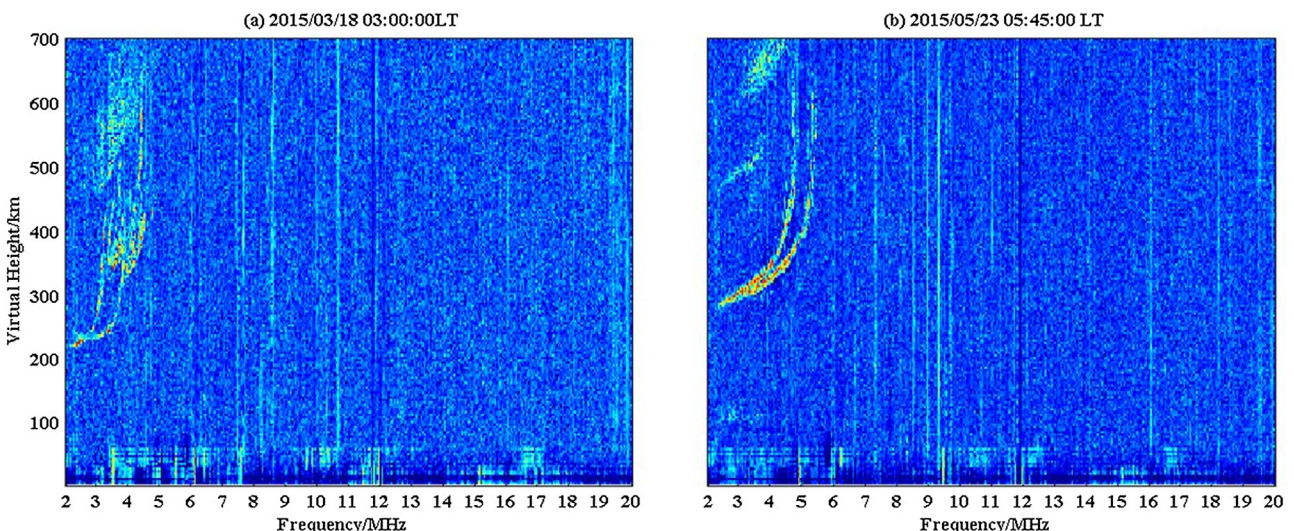


Fig. 7. Ionograms misidentified by decision tree: (a) Ionogram with SF misidentified as without SF; (b) Ionogram without SF misidentified as with SF.

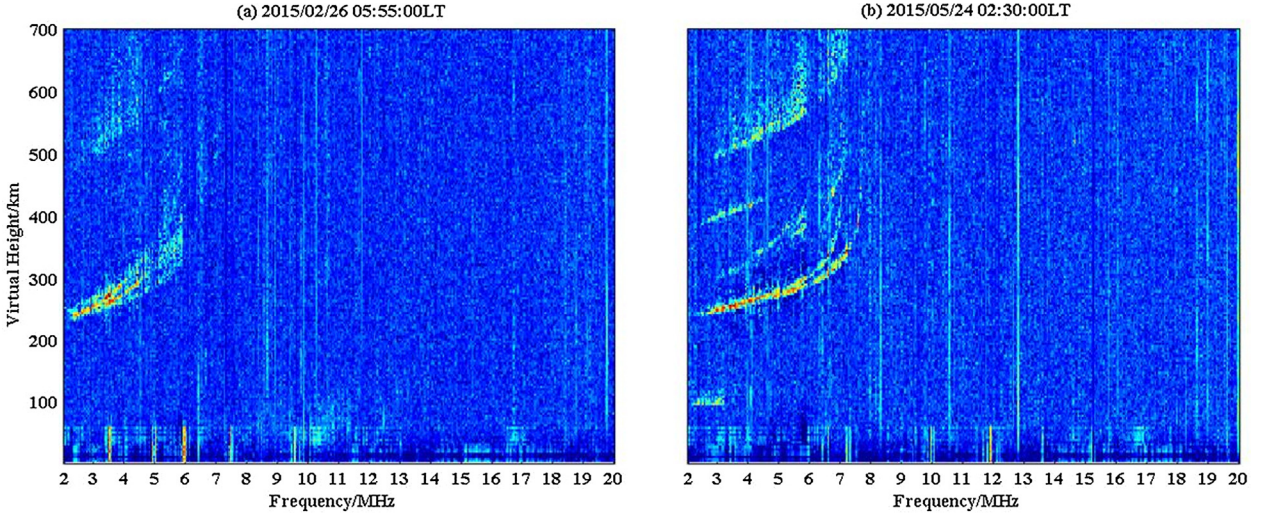


Fig. 8. Ionograms misidentified by random forest: (a) Ionogram with SF misidentified as without SF; (b) Ionogram without SF misidentified as with SF.

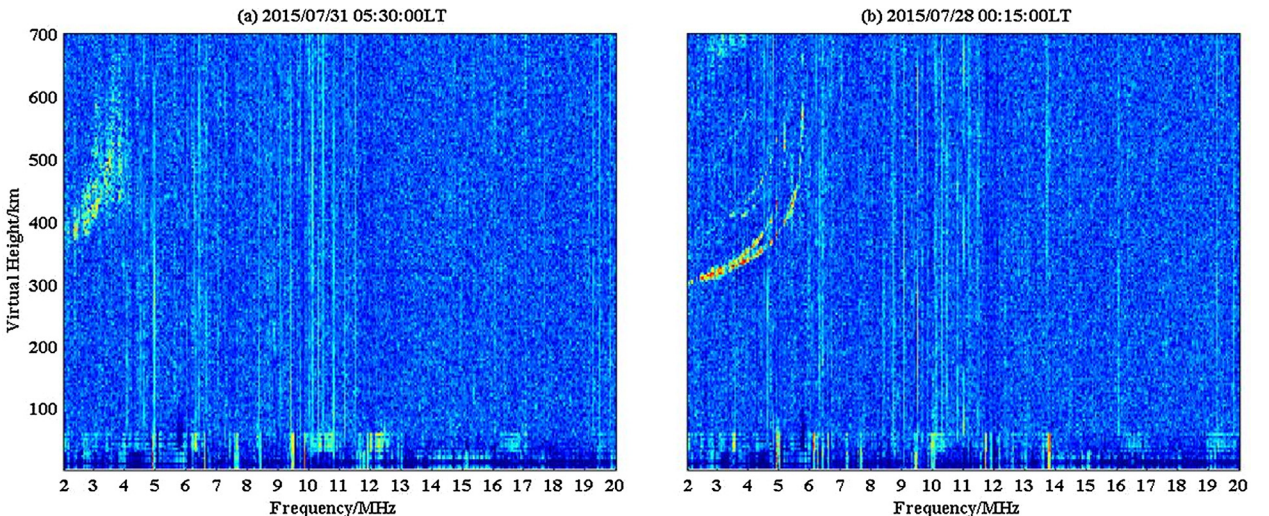


Fig. 9. Ionograms misidentified by neural network: (a) Ionogram with SF misidentified as without SF; (b) Ionogram without SF misidentified as with SF.

unbalanced sample numbers during pre-processing. A comparison shows that the neural network is more automated than the other two methods.

- (3) When the characteristics of SF must be analyzed in detail, its occurrence must be accurately identified. Since even automatic identification is capable of erroneous interpretation, one can manually confirm its results. Since there are more than 10 times as many ionograms without SF as with it, it would be daunting to search for ionograms with SF among those identified to be without it, and the opposite task would be much smaller. For this reason, the index d can be suitable to evaluate the performance of the three methods. As we can see from Table 5, the CNN have the least value of d , this confirm that CNN is the best method among the three methods.
- (4) In addition to the differences in identifying accuracy of the three method, the time spent to construct the

model varies a lot as well. The time spent depends a lot on the computer performance. We got approximately 65 min to pre-process the training data sets for decision tree and random forest using a computer with 8 GB RAM, 10 s to train a decision tree and 2 min to train the random forest model. Otherwise, we got about 200 min to train a CNN model using a computer with 32 GB RAM and GPU gtx1070. It is sure that the neural network takes much longer to train than the other methods. Moreover, because of the larger number of trees used for training, random forest takes more time to train than decision tree.

5. Summaries

Decision tree, random forest, and the deep learning method of CNN were used in the automatic classification

of SF on the same set of ionograms in this study. Results show that the accuracy of identification of ionograms with SF for all three methods can reach up to over 90%. A comparison of the identification performance of the three methods showed that the random forest method, with a slightly improved accuracy rate, was better in identifying SF than decision tree method. The neural network had significantly higher classification accuracy than the random forest method for the presence of SF, but its probability of misclassifying an ionogram without SF was also higher. Conventional machine learning methods require the manual determination of feature parameters which depend on the knowledge and experience of the researchers, and the automatic extraction of these values before training step is necessary. Since the features of ionospheric SF are relatively simple and obvious, the manual determination of the feature parameters is feasible. A relatively simple random forest method can achieve good identification results, however the neural network method extracts the parameters automatically during the training step and it requires no manual determination of the feature parameters. The random forest and decision tree methods do not require knowledge of the distribution ratios of the various classification categories in the training parameters, and the training is fast. But for the neural network method, it is preferable to know the distribution ratios of different classes to obtain a better performance, and in this case some methods are needed to reduce the sample imbalance. The neural network method also requires a longer training time, although, this training time is acceptable in the application of classification. From these aspects, the random forest method has some advantages. In summary, the CNN is more automatic, and also in consideration of the value of index d , turned out to be the best method in the classifying performance among the three methods, despite the longer training time.

Acknowledgement

This work was supported by the National Natural Science Foundation of China (NSFC 41604133), the China Postdoctoral Science Foundation funded project (2016M592374), the Fundamental Research Funds for the Central Universities, and the China Scholarship Council (201706275007). The authors acknowledge Institute of Earthquake Forecasting for providing ionosonde data.

References

- Abdu, M.A., Kherani, E.A., Batista, I.S., Paula, E.R.D., Fritts, D.C., Sobral, J.H.A., 2009. Gravity wave initiation of equatorial spread F/plasma bubble irregularities based on observational data from the SpreadFEx campaign. *Ann. Geophys.* 27 (7), 2607–2622. <https://doi.org/10.5194/angeo-27-2607-2009>.
- Bhanja, P., Earle, G.D., Bishop, R.L., Bullett, T.W., Mabie, J., Redmon, R., 2009. A statistical study of midlatitude spread F at Wallops Island, Virginia. *J. Geophys. Res. Space Phys.* 114 (A4), A04301. <https://doi.org/10.1029/2008ja013212>.
- Breiman, L., Friedman, J., Olshen, R., Stone, C., 1984. Classification and regression trees. Wadsworth, New York. <https://doi.org/10.1201/9781315139470>.
- Breiman, Leo, 1996. Bagging predictors. *Machine Learn.* 24 (2), 123–140. <https://doi.org/10.1007/bf00058655>.
- Breiman, L., 2001. Random forests. *Machine Learn.* 45 (1), 5–32. <https://doi.org/10.1023/A:1010933404324>.
- Ciresan, D.C., Meier, U., Gambardella, L.M., Schmidhuber, J., 2011. Convolutional neural network committees for handwritten character classification. In: Proceedings of the 2011 International Conference on Document Analysis and Recognition, Beijing, China, pp. 1135–1139. <https://doi.org/10.1109/ICDAR.2011.229>.
- Dungey, J.W., 1956. Convective diffusion in the equatorial F region. *J. Atmos. Terr. Phys.* 9 (5–6), 304–310. [https://doi.org/10.1016/0021-9169\(56\)90148-9](https://doi.org/10.1016/0021-9169(56)90148-9).
- Fejer, B.G., Kelley, M.C., 1980. Ionospheric irregularities. *Rev. Geophys.* 18 (2), 401–454. <https://doi.org/10.1029/RG018i002p00401>.
- Fejer, B.G., Scherliess, L., de Paula, E.R., 1999. Effects of the vertical plasma drift velocity on the generation and evolution of equatorial spread F. *J. Geophys. Res. Space Phys.* 104 (A9), 19859–19869. <https://doi.org/10.1029/1999JA900271>.
- Fawcett, T., 2006. An introduction to roc analysis. *Pattern Recognit. Lett.* 27 (8), 861–874. <https://doi.org/10.1016/j.patrec.2005.10.010>.
- Jiang, C., Yang, G., Zhou, Y., Zhu, P., Lan, T., Zhao, Z., Zhang, Y., 2017. Software for scaling and analysis of vertical incidence ionograms-*ionoScaler*. *Adv. Space Res.* 59, 968–979. <https://doi.org/10.1016/j.asr.2016.11.019>.
- Krall, J., Huba, J.D., Ossakow, S.L., Joyce, G., Makela, J.J., Miller, E. S., Kelley, M.C., 2011. Modeling of equatorial plasma bubbles triggered by non-equatorial traveling ionospheric disturbances. *Geophys. Res. Lett.* 38 (8), L08103. <https://doi.org/10.1029/2011GL046890>.
- Kingma, D.P., Ba, J.L., 2015. Adam: A method for stochastic optimization. In: Proceedings of the 3rd International Conference for Learning Representations, San Diego <https://arxiv.org/abs/1412.6980>.
- Kang, E., Min, J., Ye, J.C., 2017. A deep convolutional neural network using directional wavelets for low-dose x-ray CT reconstruction. *Med. Phys.* 44 (10), e360–e375. <https://doi.org/10.1002/mp.12344>.
- Lawrence, S., Giles, C.L., Tsoi, A.C., Back, A.D., 1997. Face recognition: a convolutional neural-network approach. *IEEE Trans. Neural Networks* 8 (1), 98–113. <https://doi.org/10.1109/72.554195>.
- LeCun, Y., Bottou, L., Bengio, Y., Haffner, P., 1998. Gradient-based learning applied to document recognition. *Proc. IEEE* 86 (11), 2278–2324. <https://doi.org/10.1109/5.726791>.
- Li, Q., Cai, W., Wang, X., Zhou, Y., Feng, D.D., Chen, M., 2014. Medical image classification with convolutional neural network. In: In Proceedings of the 2014 13th International Conference on Control Automation Robotics & Vision (ICARCV), pp. 844–848. <https://doi.org/10.1109/icarcv.2014.7064414>.
- LeCun, Y., Bengio, Y., Hinton, G., 2015. Deep learning. *Nature* 521 (7553), 436–444. <https://doi.org/10.1038/nature14539>.
- Lan, T., Zhang, Y., Jiang, C., Yang, G., Zhao, Z., 2018. Automatic identification of Spread F using decision trees. *J. Atmos. Sol. Terr. Phys.* 179, 389–395. <https://doi.org/10.1016/j.jastp.2018.09.007>.
- Martyn, D.F., 1959. Large-scale movements of ionization in the ionosphere. *J. Geophys. Res.* 64 (12), 2178–2179. <https://doi.org/10.1029/jz064i012p02178>.
- Piggot, W.R., Rawer, K., 1972. *URSI Handbook of Ionogram Interpretation and Reduction*, 2nd ed. Elsevier, New York.
- Pillat, V.G., Fagundes, P.R., Guimarães, L.N.F., 2015. Automatically identification of Equatorial Spread-F occurrence on ionograms. *J. Atmos. Sol. Terr. Phys.* 135, 118–125. <https://doi.org/10.1016/j.jastp.2015.10.015>.
- Sultan, P.J., 1996. Linear theory and modeling of the Rayleigh-Taylor instability leading to the occurrence of equatorial spread F. *J. Geophys. Res.* 101 (A12), 26875. <https://doi.org/10.1029/96JA00682>.
- Shi, S.Z., Zhao, Z.Y., Su, F.F., Chen, G., 2009. A low-power and small-size hf backscatter radar for ionospheric sensing. *IEEE Geosci.*

- Remote Sens. Lett. 6 (3), 504–508. <https://doi.org/10.1109/LGRS.2009.2020700>.
- Scotto, C., Ippolito, A., Sabbagh, D., 2018. A method for automatic detection of equatorial spread-F in ionograms. Adv. Space Res. 63 (1), 337–342. <https://doi.org/10.1016/j.asr.2018.09.019>.
- Tsunoda, R.T., 2005. On the enigma of day-to-day variability in equatorial spread F. Geophys. Res. Lett. 32 (8), 1–4. <https://doi.org/10.1029/2005GL022512>.
- Tsunoda, R.T., 2006. Day-to-day variability in equatorial spread f: is there some physics missing?. Geophys. Res. Lett. 33 (16), 423–424. <https://doi.org/10.1029/2006GL025956>.
- Woodman, R.F., Hoz, C.L., 1976. Radar observations of F region equatorial irregularities. J. Geophys. Res. 81 (31), 5447–5466. <https://doi.org/10.1029/JA081i031p05447>.